



# OPEN Effect of heavy metal copper on the physiological characteristics of *Ulva lactuca* at different temperatures

Jing Ma<sup>1</sup>, Yuxin Xie<sup>1</sup>, Wenjing Ge<sup>1</sup>, Zhouyue Lu<sup>1</sup>, Xiangwen Bao<sup>1</sup>, Houxu Ding<sup>1</sup>, Cheng Chen<sup>1</sup>, Yaping Wu<sup>1</sup>, Guoqiang Chen<sup>1</sup> & Juntian Xu<sup>1,2</sup>✉

Copper (Cu) is an essential element for macroalgae and has been extensively studied, but the interactive effects of temperature and Cu on these organisms remain less understood. In this study, we measured the photosynthetic characteristics of *Ulva lactuca* exposed to varying Cu concentrations and different temperatures (10 °C, 15 °C, and 20 °C). The results indicated that at the same temperature, as the concentration of Cu increased, the relative growth rate of *U. lactuca* showed a decreasing trend. Under three different temperatures, the photosynthetic rate and chlorophyll content of the algae significantly decreased with the increase in Cu concentration. Under the same Cu concentration conditions, as the temperature rises, the RGR of the algae gradually increases. In the case of low Cu concentration (LCu), the net photosynthetic rate at 15 °C and 20 °C increased by 103.72% and 104.97%, respectively, compared to the rate at 10 °C. Under high Cu concentration (HCu), the net photosynthetic rate at 15 °C and 20 °C increased by 192.18% and 245.67%, respectively, compared to that at 10 °C. The pigment content showed a similar trend. These results indicated that under the same temperature conditions, high concentrations of Cu inhibited the growth of algae, while under the same Cu treatment conditions, a suitable increase in temperature could alleviate the toxic effects of Cu on the algae.

**Keywords** *Ulva lactuca*, Temperature, Cu, Photosynthetic physiology

Marine heavy metal pollution refers to the contamination of the ocean caused by certain heavy metals entering through various channels. Currently, the heavy metal elements primarily polluting marine environments include Hg, Cd, Pb, Zn, Cr, and Cu. Metals such as Cu, Fe, and Zn can serve as cofactors for some proteins and enzymes; however, excessive heavy metals can lead to cellular damage. Cu is involved in a variety of metabolic processes within organisms, acting as a cofactor for at least 30 types of redox enzymes<sup>1</sup>. Research indicates that after a 7-day exposure to 100 µM Cu, the metal accumulates predominantly within the cell walls, triggering stress responses, such as leaf wilting, thylakoid membrane damage, and a decrease in the levels of photosynthetic pigments like chlorophyll a and phycobilin<sup>2</sup>. Fe, Cu, and Zn are present in enzymes that remove reactive oxygen species, which partially associate with the thylakoid membranes<sup>3</sup>.

Macroalgae are important primary producers in coastal areas, primarily found in the intertidal zone and below. They contribute approximately 10% of marine primary productivity and have significant potential for carbon dioxide fixation<sup>4–6</sup>. However, human industrial activities still rely on coal, oil, natural gas, and other fossil fuels, which will inevitably continue to emit greenhouse gases such as carbon dioxide. These gases absorb heat in the atmosphere, leading to a net increase in heat within the Earth's system, with the oceans storing over 90% of the excess heat generated by greenhouse gas emissions<sup>7</sup>. The rise in ocean temperatures impacts the salinity, pH, and dissolved oxygen levels in marine environments, subsequently affecting marine life. Against the backdrop of a significant increase in seawater temperature (average +0.80 °C), the coverage of macroalgae has declined, particularly over the past decade<sup>8</sup>.

Temperature is one of the important environmental factors affecting the growth and survival of macroalgae in the ocean. Changes in global temperatures and the specificity of habitats mean that algae are also affected by extreme environmental factors. Environmental conditions such as seawater temperature, nutrient levels, and wave erosion in intertidal zones significantly impact the rise and distribution of macroalgae<sup>9,10</sup>. Different types of algae have varying optimal temperature ranges, and the ideal growth temperature of macroalgae is related to the geographical area in which they are found<sup>11</sup>. Research indicates that when the temperature is below 25 °C,

<sup>1</sup>Jiangsu Key Laboratory of Marine Bioresources and Environment, Jiangsu Ocean University, Lianyungang 222005, China. <sup>2</sup>Co-Innovation Center of Jiangsu Marine Bio-industry Technology, Lianyungang 222005, China. ✉email: jtxu@jou.edu.cn

the absorption rate of ammonia nitrogen increases with rising temperatures<sup>12</sup>. When the temperature is lower than 25 °C, the growth rate of *Sargassum horneri*, *Ulva lactuca*, and *Sargassum fusiforme* increases with the temperature increases, but when the temperature is higher than 25 °C, the growth stops and decay appears<sup>13</sup>. Research shows that algae have a stronger antioxidant system under low-temperature stress. The photosynthetic components in their photosystem II (PSII), including the light-harvesting antenna, reaction center, electron donor side, and receptor side, can be damaged to varying degrees under low-temperature conditions, which also leads to a reduction in the expression levels of related proteins<sup>14</sup>. During high temperatures, algae activate heat shock responses that can harm the cellular membrane system, impacting enzyme activity and chlorophyll synthesis within the cells<sup>15</sup>. The photosynthetic activity of algae cultured under both low and high temperatures may also be suppressed and compensated via different mechanisms involving photosystem I (PSI) and mitochondrial oxidative phosphorylation<sup>16</sup>.

However, research on the effects of Cu at different temperatures on macroalgae, such as *U. lactuca*, is relatively scarce, providing an important entry point for our studies. *Ulva lactuca* belongs to the green algae division and is an important marine alga. It plays a crucial role in ecosystems, such as carbon fixation and oxygen release, and due to its rich nutritional components, it has extensive applications in agriculture, medicine, food, and industry<sup>17</sup>. As people increasingly focus on nutrition and health, the market demand for *U. lactuca* has been gradually rising, making it particularly important to explore its ability to adapt to different environmental conditions. Our current hypothesis is that temperature variations may significantly affect the growth and physiological processes of photosynthesis in *U. lactuca*, laying the groundwork for in-depth research. The main aim of this experiment is to investigate the effects of Cu on the growth, photosynthetic physiology, and chlorophyll fluorescence parameters of *U. lactuca* under different temperature conditions. By conducting Cu pollution experiments at varying temperatures, we can observe *U. lactuca*'s response mechanisms to heavy metal Cu under different thermal conditions, specifically including changes in growth rate, photosynthetic efficiency, chlorophyll content, and chlorophyll fluorescence characteristics. This will not only help us understand *U. lactuca*'s adaptability to environmental stress but also reveal the vulnerability and resilience of marine ecosystems in the face of pollution and climate change.

## Materials and methods

### Algal samples

*Ulva lactuca* were collected from the intertidal zone in Qingdao, Shandong Province, China, in May 2023, and were subsequently transported back at 4 °C to the laboratory. To remove sediment and epiphytic algae, the samples were washed thoroughly with sterilized seawater. Healthy algal specimens were then cultured in sterilized seawater supplemented with 60 µM NaNO<sub>3</sub> and 8.0 µM NaH<sub>2</sub>PO<sub>4</sub> to meet the nutritional requirements for their normal growth at 150 µmol photons m<sup>-2</sup> s<sup>-1</sup> of 20 °C, with a light/dark cycle of 12:12 h. The culture medium was renewed every 2 days.

### Experimental design

After 3 days of pre-cultivation, 0.05 g of the algae was transferred into a flask containing 500 mL of sterilized seawater and cultured under aeration in a GXZ-300C intelligent lighting incubator, following the research methods described by Wang et al.<sup>18</sup>. The sterilized seawater was similarly enriched with 60 µM NaNO<sub>3</sub> and 8.0 µM NaH<sub>2</sub>PO<sub>4</sub> to ensure the algae had adequate nutrition for normal growth<sup>19</sup>. The experiment used three different Cu concentrations (natural seawater, LCu; 16 µg L<sup>-1</sup>, MCu; 32 µg L<sup>-1</sup>, HCu) and temperatures (10 °C, 15 °C, and 20 °C) to explore their effects on algal growth and photosynthetic physiological characteristics. Cu concentration was selected based on the concentration of Cu found in the Bohai Sea and Port Adelaide, South Australia, with a Cu concentration of 1.92 µg L<sup>-1</sup> and 64.64 µg L<sup>-1</sup>, respectively<sup>20,21</sup>. Natural seawater from the Yellow Sea without added CuSO<sub>4</sub> (Cu concentration of 1.28 µg L<sup>-1</sup>) was used as a control (low Cu treatment). Analysis was conducted using a flame-less graphite furnace atomic absorption spectrometer<sup>22</sup>. The optimal growth temperature for *U. lactuca* is between 15 and 20 °C<sup>23</sup>. However, factors such as extreme weather conditions, water depth, and seasonal fluctuations often lead to temperature variations in spring and autumn. Based on this, the culture temperatures were set to 10 °C, 15 °C, and 20 °C, respectively. The light intensity and light/dark cycle remained consistent with those used during pre-cultivation, and the sterilized seawater was also replaced every 2 days. After the relative growth rate (RGR), was measured every 2 days, and stabilized after 1 week of cultivation, the rate of photosynthesis, respiration rate, chlorophyll content, and fluorescence parameters were measured.

### Measure of growth

RGR was calculated every 2 days by weighing the algae after removing surface moisture with a paper towel to measure the fresh weight. The RGR was calculated according to Ma et al.<sup>19</sup>.

### Measurement of the rates of photosynthesis and respiration

The net photosynthesis and respiration rates of thalli were measured by a Clark-type oxygen electrode (YSI Model 5300A, USA). The algae were cut into approximately 1 cm squares, and 0.02 g samples were placed into a reaction chamber containing 8 mL of culture seawater. 150 µmol photons m<sup>-2</sup> s<sup>-1</sup> were used in this experiment, with the temperature set to that of the respective algal treatments. The samples were dark-adapted in the reaction chamber for 5 min, during which the initial values were recorded. Measurements were taken every 60 s until the difference stabilized, and the decrease in O<sub>2</sub> was used to calculate the respiration rate. Following this, the net photosynthesis rate was measured under culture light intensity and temperature, using the same experimental procedure as for the respiration rate. The calculation formula is according to Xu et al.<sup>23</sup> as follows:

$$P = 60 \times a \times d \times V/m$$

where *a* represents the oxygen solubility of seawater at different culture temperatures, *d* represents the difference of change of O<sub>2</sub> per minute, *V* represents the volume of seawater in the reaction chamber, and *m* represents the fresh weight of the algae.

**Chlorophyll fluorescence measurements**

Fluorescence parameters of the thalli were determined using a chlorophyll fluorescence instrument (AP100-C). After subjecting the algae samples to dark adaptation for 20 min, they were placed in plastic cuvettes. The actinic light was set to simulate growth light intensity, allowing for the measurement of relative electron transport rate (rETR), light response curves, and rapid fluorescence kinetic curves (OJIP), from which radar plot-related data were calculated (Table 1).

$$rETR \left( \mu\text{mol e}^{-1} \text{ m}^{-2} \text{ s}^{-1} \right) = 0.5 \times \text{Yield} \times \text{PAR}$$

The yield indicates the effective photochemical quantum yield of PSII in response to illumination, with 0.5 representing the percentage of absorbed light relative to the total incident light. The PAR indicates the intensity of the photochemical light. After exposure to six different light intensities (0, 200, 400, 600, 800, and 1000 150 μmol photons m<sup>-2</sup> s<sup>-1</sup>), the light response curve of thalli was measured, and the maximum relative electron transport rate (rETR<sub>max</sub>), light utilization efficiency (α), and light saturation intensity (I<sub>k</sub>) were obtained through curve fitting<sup>24,25</sup>.

**Determination of the pigment content**

About 0.02 g algal sample was treated in the dark at 4 °C with 10 mL of anhydrous methanol for 24 h to extract the chlorophyll. The absorbance of the samples was measured at 652 nm, and 665.2 nm using a UV-visible spectrophotometer (Ultravist 3300 Pro, Amersham Biosciences Ltd. Sweden). The contents of chlorophyll (Chl *a*) and Chl *b* were calculated according to the methodology described by Porra et al.<sup>26</sup>.

**Data analysis**

The results were expressed as the mean ± standard deviation. Data were processed using Origin 9.0 software, three replicates were taken for each treatment. A 95% confidence interval was set for all tests. Lowercase letters represent the significant difference among the Cu concentrations at the same temperature (*P* < 0.05). Uppercase letters represent the significant difference among the temperatures at the same Cu concentration (*P* < 0.05). Visualization of the clustering heat map analysis of growth and photosynthetic physiological parameters was performed using TBtools software<sup>27</sup>.

Terms and formulas	Illustrations
$V_j = (F_j - F_0)/(F_M - F_0)$	Relative variable fluorescence at phase J of the fluorescence induction curve
$V_i = (F_i - F_0)/(F_M - F_0)$	Relative variable fluorescence at phase I of the fluorescence induction curve
$M_0$	Net rate of PSII closure
$F_M$	Maximum value under saturating illumination
$F_0$	First reliable fluorescence value after the onset of actinic illumination; used as the initial value of the fluorescence
$F_v/F_M$	Maximum quantum yield of PSII photochemistry
$\Phi P_0 = TR_0/ABS = F_v/F_M = [1 - (F_0/F_M)]$	Maximum quantum yield of primary photochemistry
$\Phi E_0 = ET_0/ABS = [1 - (F_0/F_M)] \times (1 - V_j)$	Quantum yield of electron transport
$\Psi_0 = 1 - V_j$	Efficiency with which a trapped exaction can move an electron into the electron transport chain further than Q <sub>A</sub>
$\Phi D_0 = DI_0/ABS = 1 - \Phi P_0 = (F_0/F_M)$	Thermal dissipation quantum yield
$\Phi R_0 = \Phi P_0 \Psi E_0 \delta R_0$	Quantum yield of reduction of end electron acceptors of PSI
$ABS/RC = (M_0/V_j)/(1 - (F_0/F_M))$	Light absorption flux (for PSII antenna chlorophylls) per reaction center (RC)
$DI_0/RC = ABS/RC - TR_0/RC$	Dissipation energy flux per PSII RC (at <i>t</i> = 0)
$ET_0/RC = (M_0/V_j) \times (1 - V_j)$	Maximum electron transport flux (further than Q <sub>A</sub> <sup>-</sup> ) per PSII RC (at <i>t</i> = 0)
$TR_0/RC = (M_0/V_j)$	Trapped (maximum) energy flux (leading to Q <sub>A</sub> reduction) per RC (at <i>t</i> = 0)
$RE_0/RC = M_0(1/V_j) (1 - V_j)$	Electron flux reducing end electron acceptors at the PSI acceptor side per RC
$ABS/CSm = F_M$	Absorption flux of photons per cross section, approximated by F <sub>M</sub>
$TR_0/CSm = \Phi P_0 \times (ABS/CSm)$	Phenomenological fluxes for trapping per cross section, approximated by F <sub>M</sub>
$ET_0/CSm = \Phi E_0 \times (ABS/CSm)$	Potential electron transport per cross section, approximated by F <sub>M</sub>
$DI_0/CSm = (ABS/CSm) - (TR_0/CSm)$	Dissipation per cross section, approximated by F <sub>M</sub>

**Table 1.** OJIP transient parameters related to JIP-test.

## Results

### Growth rates

At 10 °C, compared to LCu, the RGR of thalli under MCu and HCu decreased by 23.85% and 52.09%, respectively ( $P < 0.05$ ) (Fig. 1). At 15 °C, compared to LCu, the RGR in MCu and HCu conditions decreased by 22.38% and 32.95%, respectively ( $P < 0.05$ ); at 20 °C, compared to LCu, the RGR in HCu conditions decreased by 26.96% ( $P < 0.05$ ). When comparing RGR under LCu at 10 °C, the rates increased by 53.08% and 65.89% at 15 °C and 20 °C, respectively ( $P < 0.05$ ). For MCu, at 10 °C, RGR increased by 55.92% and 113.66% at 15 °C and 20 °C, respectively ( $P < 0.05$ ). Under HCu, when compared to the RGR at 10 °C, the rates increased by 114.22% and 152.88% at 15 °C and 20 °C, respectively ( $P < 0.05$ ).

### Photosynthesis and respiration rates

At 10 °C, compared to LCu, the net photosynthetic rate of the thalli decreased by 35.22% and 51.94% under MCu and HCu, respectively ( $P < 0.05$ ) (Fig. 2A). At 15 °C, compared to LCu, the net photosynthetic rate increased by 8.36% under MCu ( $P < 0.05$ ), while it decreased by 31.07% under HCu ( $P < 0.05$ ); at 20 °C, the net photosynthetic rate decreased by 18.95% under HCu compared to LCu ( $P < 0.05$ ). In the case of LCu, the net photosynthetic rates increased by 103.72% and 104.97% at 15 °C and 20 °C, respectively, compared to the rate at 10 °C ( $P < 0.05$ ). Under MCu, the net photosynthetic rates increased by 240.79% and 242.55% at 15 °C and 20 °C compared to 10 °C, respectively ( $P < 0.05$ ). Under HCu, when compared to the net photosynthetic rate at 10 °C, the rates increased by 192.18% and 245.67% at 15 °C and 20 °C, respectively ( $P < 0.05$ ).

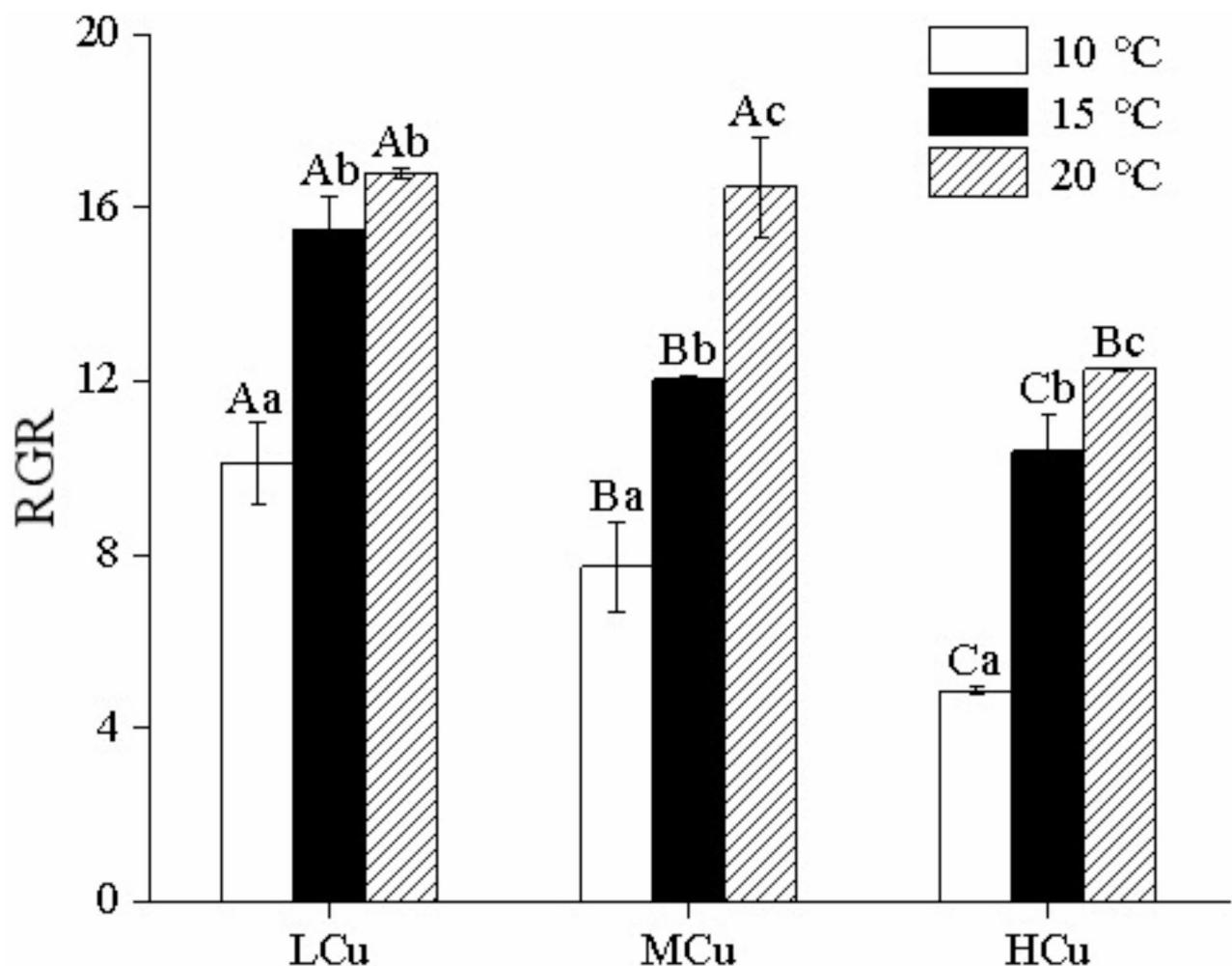


**Fig. 1.** Relative growth rate of *U. lactuca* at different temperatures (10 °C, 15 °C, and 20 °C) and Cu concentrations (natural seawater, LCu; 16  $\mu\text{g L}^{-1}$ , MCu; 32  $\mu\text{g L}^{-1}$ , HCu). Values represent the mean  $\pm$  SD ( $n = 3$ ). Different letters represent significant differences ( $P < 0.05$ ) between different Cu concentrations at the same  $\text{CO}_2$  concentration. Uppercase letters indicate the analysis of variance for each parameter under different Cu concentrations at the same temperature, while lowercase letters indicate the analysis of variance for each parameter under different temperatures at the same Cu concentration. The horizontal line indicated significant differences among  $\text{CO}_2$  concentrations while maintaining the same Cu concentrations ( $P < 0.05$ ).

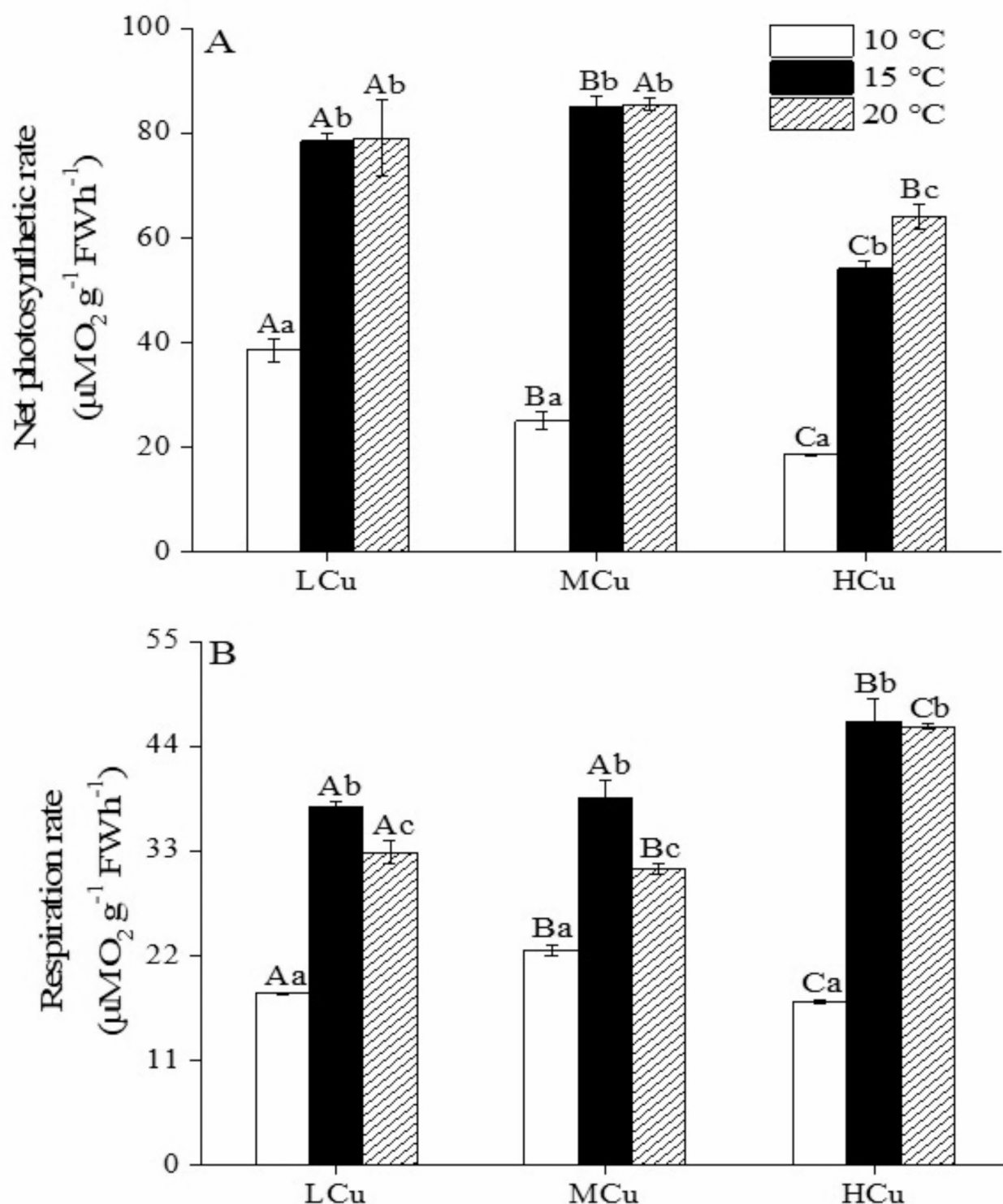


**Fig. 2.** Photosynthetic rate (A) and respiration rate (B) of *U. lactuca* at different temperatures (10 °C, 15 °C, and 20 °C) and Cu concentrations (natural seawater, LCu; 16  $\mu\text{g L}^{-1}$ , MCu; 32  $\mu\text{g L}^{-1}$ , HCu). Values represent the mean  $\pm$  SD ( $n = 3$ ). Different letters represent significant differences ( $P < 0.05$ ) between different Cu concentrations at the same  $\text{CO}_2$  concentration. Uppercase letters indicate the analysis of variance for each parameter under different Cu concentrations at the same temperature, while lowercase letters indicate the analysis of variance for each parameter under different temperatures at the same Cu concentration. The horizontal line indicated significant differences among  $\text{CO}_2$  concentrations while maintaining the same Cu concentrations ( $P < 0.05$ ).



At 10 °C, compared to LCu, the respiratory rate of thalli increased by 25.14% under MCu ( $P < 0.05$ ), while it decreased by 4.75% under HCu ( $P < 0.05$ ) (Fig. 2B). At 15 °C, compared to LCu, the respiratory rate increased by 23.97% under HCu ( $P < 0.05$ ); at 20 °C, compared to LCu, the respiratory rate decreased by 5.31% under MCu and increased by 40.31% under HCu ( $P < 0.05$ ). In LCu conditions, respiratory rates increased by 108.87% and 82.40% at 15 °C and 20 °C, respectively, compared to that at 10 °C ( $P < 0.05$ ). Under MCu, the respiratory rates increased by 71.27% and 38.01% at 15 °C and 20 °C compared to 10 °C, respectively ( $P < 0.05$ ). Under HCu, when compared to the respiratory rate at 10 °C, the rates increased by 171.83% and 168.68% at 15 °C and 20 °C, respectively ( $P < 0.05$ ).

### Chlorophyll fluorescence parameters

At 10 °C, no significant difference was observed in the maximum relative electron transport rate ( $rETR_{max}$ ) of thalli compared to LCu under MCu and HCu conditions ( $P > 0.05$ ) (Fig. 3 and Table 2). At 15 °C,  $rETR_{max}$  decreased by 22.50% and 31.42% under MCu and HCu conditions, respectively, compared to LCu ( $P < 0.05$ ); at 20 °C,  $rETR_{max}$  decreased by 18.00% and 26.93% under MCu and HCu conditions, respectively, compared to LCu ( $P < 0.05$ ). In LCu,  $rETR_{max}$  increased by 86.39% and 278.86% at 15 °C and 20 °C, respectively, compared to  $rETR_{max}$  at 10 °C ( $P < 0.05$ ). Under MCu,  $rETR_{max}$  increased by 59.33% and 242.69% at 15 °C and 20 °C, respectively, compared to 10 °C ( $P < 0.05$ ). Under HCu,  $rETR_{max}$  increased by 31.00% and 183.73% at 15 °C and 20 °C, respectively, compared to 10 °C ( $P < 0.05$ ).

At 10 °C, the efficiency of electron transport ( $\alpha$ ) of thalli increased by 42.86% under HCu compared to LCu ( $P < 0.05$ ) (Fig. 3 and Table 2). At 15 °C, there was no significant difference in  $\alpha$  between MCu and HCu compared to LCu ( $P > 0.05$ ); however, at 20 °C,  $\alpha$  decreased by 17.91% under MCu compared to LCu ( $P < 0.05$ ). In LCu,  $\alpha$  increased by 52.38% and 219.05% at 15 °C and 20 °C, respectively, compared to  $\alpha$  at 10 °C ( $P < 0.05$ ). Under MCu,  $\alpha$  increased by 139.13% at 20 °C compared to 10 °C ( $P < 0.05$ ). Under HCu,  $\alpha$  increased by 3.33% and 110% at 15 °C and 20 °C, respectively, compared to 10 °C ( $P < 0.05$ ).

At 10 °C, the saturating irradiance ( $I_k$ ) decreased by 30.34% under HCu compared to LCu ( $P < 0.05$ ) (Fig. 3 and Table 2). At 15 °C,  $I_k$  decreased by 22.92% and 27.98% under MCu and HCu conditions, respectively, compared to LCu ( $P < 0.05$ ); at 20 °C,  $I_k$  decreased by 22.11% under HCu compared to LCu ( $P < 0.05$ ). In LCu,  $I_k$  increased by 21.59% and 19.98% at 15 °C and 20 °C, respectively, compared to  $I_k$  at 10 °C ( $P < 0.05$ ). Under MCu,  $I_k$  increased by 45.17% at 20 °C compared to 10 °C ( $P < 0.05$ ). Under HCu, there was no significant difference in  $I_k$  at 15 °C and 20 °C compared to 10 °C ( $P > 0.05$ ).

### Chlorophyll *a* fluorescence OJIP transient curves and spider plots of JIP parameters

At 10 °C, the J, I, and P phase values of LCu were higher than those of MCu and HCu, with similar increases in the J, I, and P phase values of MCu and HCu. At 15 °C, the P phase value of LCu was higher than that of MCu and HCu, with the J and I phase increases of MCu being similar to those of LCu, while the J, I, and P phases of HCu were the lowest. At 20 °C, the J, I, and P phase values of LCu were the highest, and the J, I, and P phases of MCu and HCu showed a similar upward trend (Fig. 4).

Based on the parameters derived from the OJIP curve, relevant fluorescence parameter values were calculated, resulting in a radar chart (Table 1 and Fig. 5). From the chart, it could be observed that at 10 °C, the ABS/RC, DIO/RC, and REO/RC of MCu were higher than those of LCu and HCu. At 15 °C, the ETO/CSm, TRO/CSm, DIO/CSm, and ABS/CSm of HCu were significantly higher than those of LCu and MCu. At 20 °C, the  $\Phi Ro$  and REO/RC of HCu reached their lowest values, while the ABS/RC, TRO/RC, ETO/RC, and REO/RC of MCu reached their highest values, indicating that under HCu conditions, the algal cells absorbed more energy but failed to dissipate it completely, resulting in some damage to the algal cells.

### Pigment contents

At 10 °C, compared to LCu, the Chl *a* of thalli decreased by 8.58% under high copper concentration (HCu) ( $P < 0.05$ ) (Fig. 6A). At 15 °C, compared to LCu, the Chl *a* of thalli decreased by 8.04% under HCu conditions. At 20 °C, compared to LCu, the Chl *a* of thalli decreased by 10.98% and 16.59% under MCu and HCu conditions respectively ( $P < 0.05$ ). When under LCu, the Chl *a* of the algae increased by 22.39% and 43.92% at 15 °C and 20 °C respectively compared to the Chl *a* at 10 °C ( $P < 0.05$ ). Under MCu, the Chl *a* of the algae increased by 24.34% and 37.68% at 15 °C and 20 °C respectively compared to the Chl *a* at 10 °C ( $P < 0.05$ ). Under HCu, the Chl *a* of the algae increased by 23.12% and 31.31% at 15 °C and 20 °C respectively compared to the Chl *a* at 10 °C ( $P < 0.05$ ).

At 10 °C, there was no significant difference in Chl *b* of thalli under MCu and HCu compared to LCu ( $P > 0.05$ ) (Fig. 6B). At 15 °C, compared to LCu, the Chl *b* of thalli decreased by 6.40% and 8.98% under MCu and HCu conditions respectively ( $P < 0.05$ ); at 20 °C, compared to LCu, the Chl *b* of thalli decreased by 11.03% and 22.01% under MCu and HCu conditions respectively ( $P < 0.05$ ). Under LCu, the Chl *b* of the thalli increased by 11.02% and 33.53% at 15 °C and 20 °C respectively compared to the Chl *b* at 10 °C ( $P < 0.05$ ). Under MCu, the Chl *b* of the thalli increased by 11.94% and 27.97% at 15 °C and 20 °C respectively compared to the Chl *b* at 10 °C ( $P < 0.05$ ). Under HCu, there was no significant difference in Chl *b* of the algae at 15 °C and 20 °C compared to the Chl *b* at 10 °C ( $P > 0.05$ ).

At 10 °C and 15 °C, there was no significant difference in the Chl *a/b* ratio of thalli under MCu compared to LCu ( $P > 0.05$ ) (Fig. 6C). At 20 °C, compared to LCu, the Chl *a/b* ratio of Ulva increased by 7.09% under HCu conditions ( $P < 0.05$ ). Under LCu, the Chl *a/b* ratio of the algae increased by 10.25% and 7.65% at 15 °C and 20 °C respectively compared to the Chl *a/b* ratio at 10 °C ( $P < 0.05$ ). Under MCu, there was no significant difference in the Chl *a/b* ratio of the algae at 15 °C and 20 °C compared to the Chl *a/b* ratio at 10 °C ( $P > 0.05$ ). Under HCu, the Chl *a/b* ratio of the algae increased by 18.26% and 22.38% at 15 °C and 20 °C respectively compared to the Chl *a/b* ratio at 10 °C ( $P < 0.05$ ).

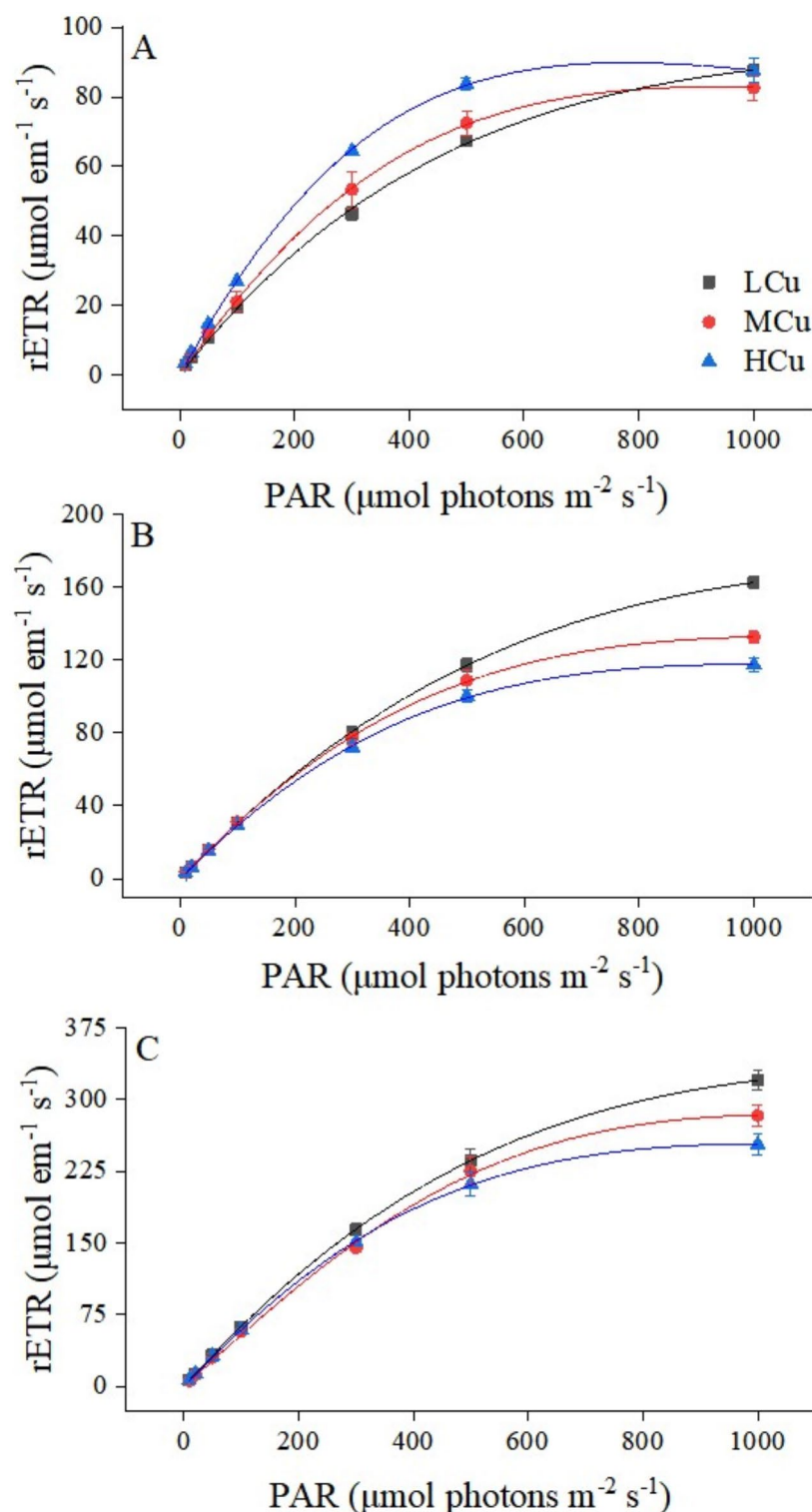


**Fig. 3.** The rapid light curve of *U. lactuca* at different temperatures (10 °C, 15 °C, and 20 °C) and Cu concentrations (natural seawater, LCu; 16  $\mu\text{g L}^{-1}$ , MCu; 32  $\mu\text{g L}^{-1}$ , HCu).

### Cluster heatmap analysis

Through cluster heatmap analysis (Fig. 7), the physiological and photosynthetic parameters of *U. lactuca* under different temperatures (LT: 10 °C, MT: 15 °C, HT: 20 °C) and Cu concentrations (LCu, MCu, and HCu) showed significant clustering differences, categorized into two functional groups: (1) Growth and photosynthesis-related parameters: including maximum relative electron transport rate ( $rETR_{\text{max}}$ ), electron transport efficiency ( $\alpha$ ), saturation irradiance ( $I_k$ ), net photosynthetic rate, relative growth rate (RGR), Chl *a*, and Chl *b* content. (2) Stress

	rETR <sub>max</sub>	α	I <sub>k</sub>
10 °C-LCu	92.06 ± 7.42 <sup>Aa</sup>	0.21 ± 0.01 <sup>Aa</sup>	436.45 ± 6.53 <sup>Aa</sup>
10 °C-MCu	83.46 ± 2.63 <sup>Aa</sup>	0.23 ± 0.03 <sup>Aa</sup>	362.20 ± 55.18 <sup>ABa</sup>
10 °C-HCu	89.82 ± 2.94 <sup>Aa</sup>	0.30 ± 0.00 <sup>Ba</sup>	304.01 ± 14.63 <sup>Ba</sup>
15 °C-LCu	171.59 ± 2.38 <sup>Ab</sup>	0.32 ± 0.01 <sup>Ab</sup>	530.68 ± 14.55 <sup>Ab</sup>
15 °C-MCu	132.98 ± 2.99 <sup>Bb</sup>	0.33 ± 0.00 <sup>Aa</sup>	409.05 ± 8.07 <sup>Bab</sup>
15 °C-HCu	117.67 ± 3.85 <sup>Cb</sup>	0.31 ± 0.04 <sup>Ab</sup>	382.20 ± 59.35 <sup>Ba</sup>
20 °C-LCu	348.78 ± 38.67 <sup>Ac</sup>	0.67 ± 0.05 <sup>Ac</sup>	523.64 ± 32.58 <sup>Ab</sup>
20 °C-MCu	286.01 ± 10.87 <sup>Bc</sup>	0.55 ± 0.04 <sup>Bb</sup>	525.81 ± 56.59 <sup>Ab</sup>
20 °C-HCu	254.85 ± 12.76 <sup>Bc</sup>	0.63 ± 0.06 <sup>ABb</sup>	407.85 ± 55.59 <sup>Ba</sup>

**Table 2.** The maximum relative electron transport rate (rETR<sub>max</sub>), the efficiency of electron transport (α), and the saturating irradiance (I<sub>k</sub>) of the rapid light curve of *U. lactuca* at different temperatures (10 °C, 15 °C, and 20 °C) and Cu concentrations (natural seawater, LCu; 16 µg L<sup>-1</sup>, MCu; 32 µg L<sup>-1</sup>, HCu). Different letters represent significant differences (*P* < 0.05) between different Cu concentrations at the same CO<sub>2</sub> concentration. Uppercase letters indicate the analysis of variance for each parameter under different Cu concentrations at the same temperature, while lowercase letters indicate the analysis of variance for each parameter under different temperatures at the same Cu concentration. Values represent the mean ± SD (n = 3).

response parameters: respiration rate and Chl *a/b* ratio. For growth and photosynthetic parameters, under LT-HCu, the net photosynthetic rate (color bar value close to -2) and rETR<sub>max</sub> (value -1.8) significantly decreased. The RGR (value -2.0) reached its lowest level. At HT-MCu, the photosynthetic efficiency peaked, with the net photosynthetic rate (value close to 2) reaching its maximum. Under HT-LCu, the RGR (value close to 1) was significantly higher than other high-temperature treatments. For stress response parameters, the respiration rate in the MT-HCu group sharply increased (value 2). In the HT-HCu group, the respiration rate also rose (value 1.5), but photosynthetic parameters collapsed entirely. The Chl *a/b* ratio was highest in the HT-HCu group (value 1.5). Conversely, the LT-HCu group showed a lower Chl *a/b* ratio (value -2). For interactive effects of temperature and Cu, all low-temperature treatments (LT-LCu, LT-MCu, LT-HCu) exhibited significantly reduced I<sub>k</sub> and Chl *b* content, with weak Cu concentration effects. In the HT-HCu group, parameters such as net photosynthetic rate, RGR, rETR<sub>max</sub>, α, and Chl *a/b* ratio deteriorated (values mostly below -1.5), while the respiration rate peaked. The MT-MCu group showed intermediate parameter values (e.g., net photosynthetic rate near 0), indicating that moderate temperature partially alleviated Cu toxicity, though medium Cu still caused mild photosynthetic inhibition.

Discussion

Photosynthesis is a complex metabolic activity in living organisms; it is a biological pathway that can convert light energy and is also an important component of the Earth's carbon cycle. Macroalgae can concentrate heavy metals to a significant extent. Generally, the accumulation of specific metals in plants depends on their uptake ability and the functionality of intracellular binding sites<sup>28</sup>. The cell wall of plant cells contains proteins and carbohydrates that can bind with metal ions. When the binding sites on the cell wall become saturated with metal ions, heavy metal ions from metabolic processes can accumulate in large quantities within the cell, potentially leading to toxic effects that impact cell growth and metabolism<sup>29</sup>. Growth is the comprehensive manifestation of photosynthesis in algae under heavy metal stress<sup>30</sup>. The results of this study show that at the same temperature, the RGR of thalli declined as the concentration of Cu increased. At 10 °C, the decrease in growth rate in the HCu condition compared to the LCu condition was the most pronounced, indicating that the growth was inhibited by the increase in Cu concentration. This is consistent with the findings of Kondzior and Butarewicz<sup>31</sup>, who observed that under increasing Cu concentrations, *Chlorella vulgaris* continued to grow, but its growth was significantly inhibited. Bajguz<sup>32</sup> also noted that heavy metals could suppress the growth of *Chlorella vulgaris*. Han et al.<sup>33</sup> compared the Cu tolerance of two green algae species *Ulva pertusa* and *U. armoricana*. They found that exposure to Cu concentrations of 25–50 µg L<sup>-1</sup> did not affect the growth of *U. armoricana*, but the growth of *U. pertusa* was significantly reduced. The difference in Cu sensitivity between the two algae species could influence their survival in coastal waters, thereby affecting the composition of coastal communities. Under the same Cu conditions, with the temperature increased, the RGR of the algal gradually rose. When at relatively low temperatures, the RGR increased with rising temperature, showing significant differences, which indicated that higher temperatures alleviate the toxic effects of Cu on algae and promote the growth of thalli. These findings were consistent with the studies by Ma et al.<sup>18</sup>. On the early life history of kelp, Leal<sup>34</sup> pointed out that while ocean warming had no significant impact on the early life history of kelp, the addition of heavy metal Cu caused a moderate negative effect on the stages of meiosis and spore germination. Cu is one of the essential trace elements for plant growth; it plays a role not only in the antioxidative mechanisms of photosynthesis but also in the catalytic processes of many enzymes that are crucial for algal growth and development. In the process of photosynthesis, Cu helps maintain the stability of the electron transport chain, thereby ensuring that algae can capture light energy and convert it into chemical energy. However, when the concentration of Cu exceeds the tolerance level of algal, it may trigger a series of adverse reactions<sup>35</sup>. Research indicated that excess Cu interfered with various physiological processes in photosynthetic cells, particularly the functions of the photoreaction



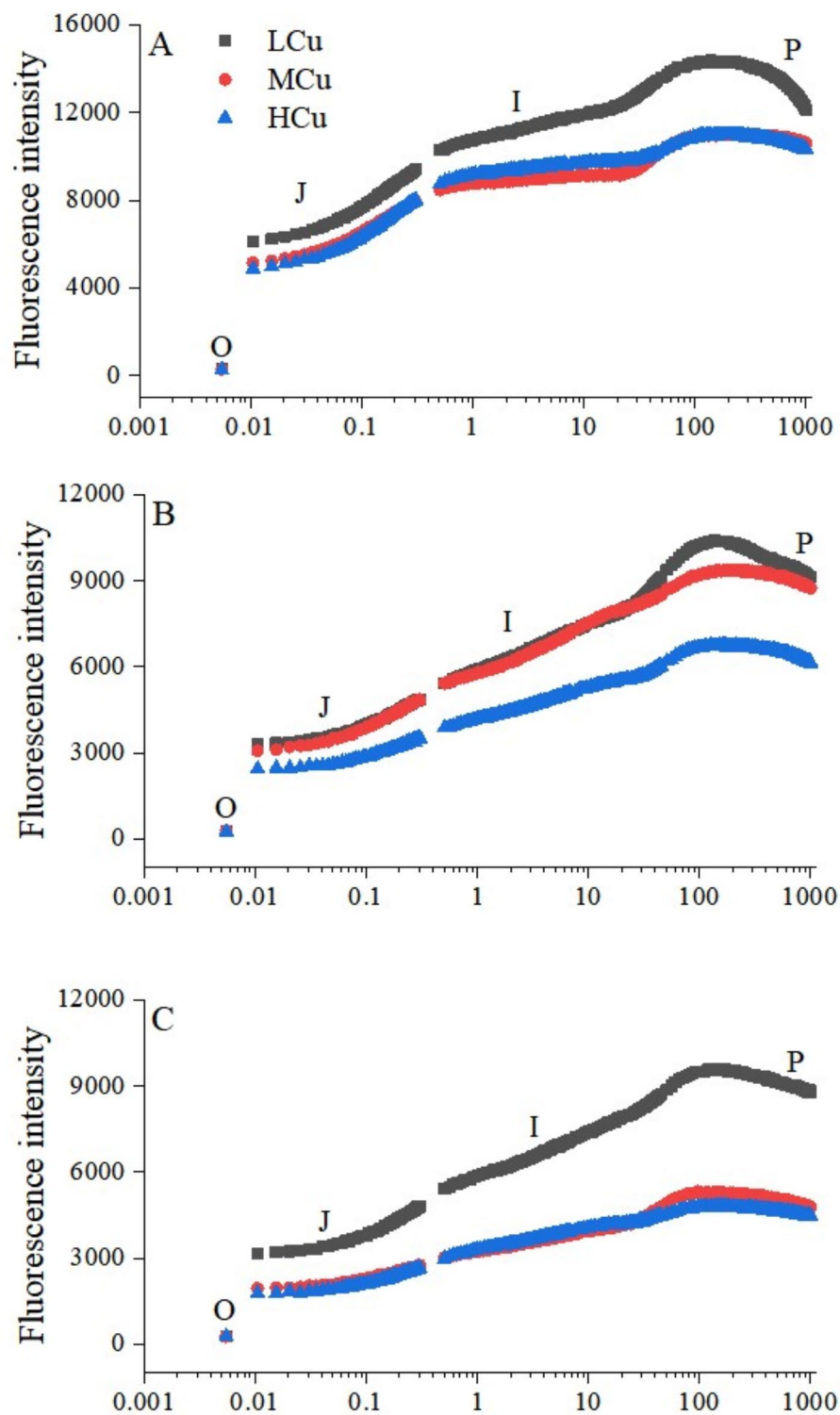


**Fig. 4.** Chlorophyll *a* fluorescence OJIP transient curves of *Ulva lactuca* at different temperatures (10 °C, 15 °C, and 20 °C) and Cu concentrations (natural seawater, LCu; 16  $\mu\text{g L}^{-1}$ , MCu; 32  $\mu\text{g L}^{-1}$ , HCu). Each step in the figure indicates the minimal fluorescence intensity when all PSII reaction centers (RC) are open (the O step), the intensity at 2 ms (the J step), the intensity at 30 ms (the I step), and the maximal intensity when all PSII RCs are closed (the P step).

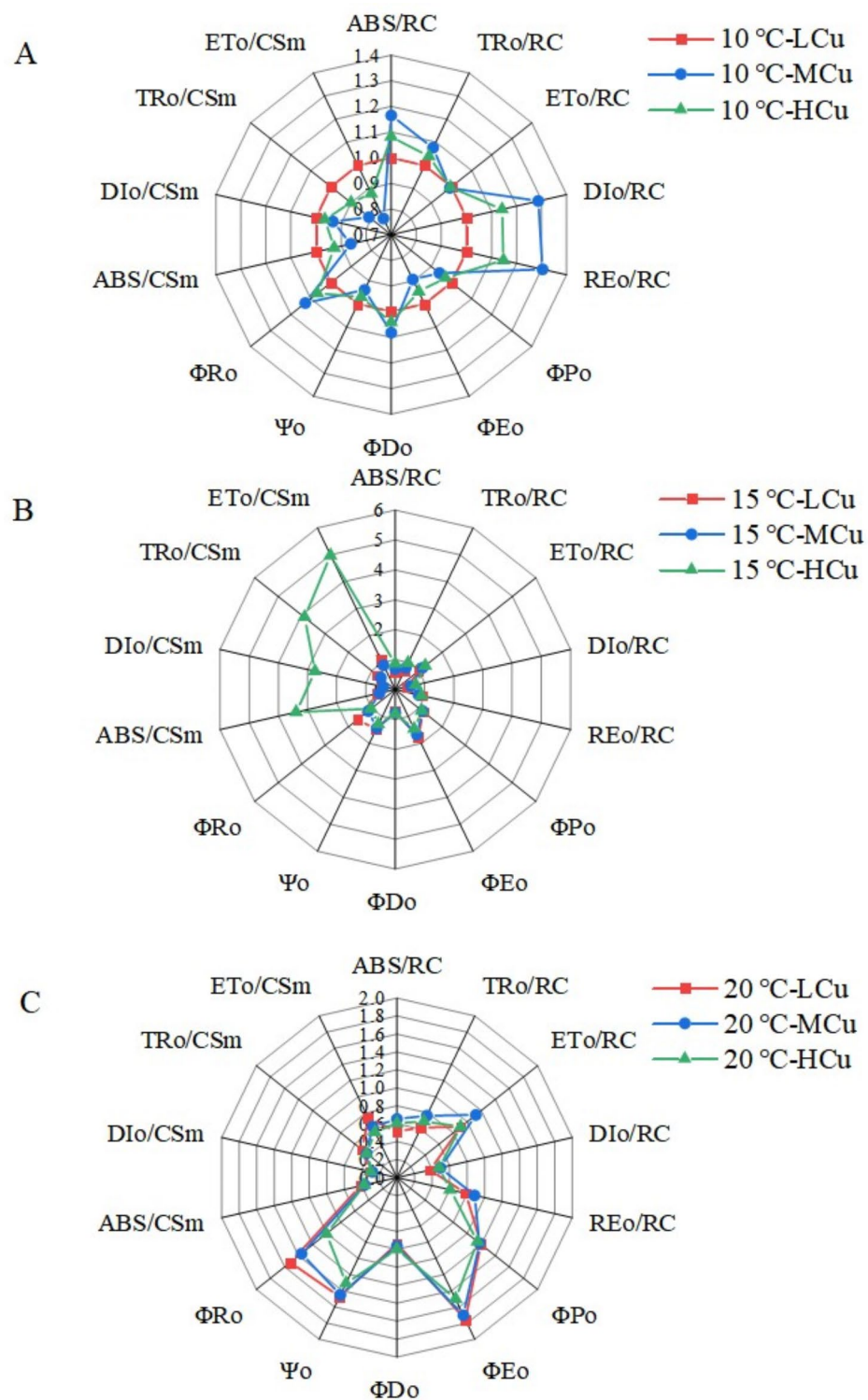


**Fig. 5.** Spider plots of JIP parameters deduced from chlorophyll *a* fluorescence OJIP transient curves of *Ulva lactuca* at different temperatures (10 °C, 15 °C, and 20 °C) and Cu concentrations (natural seawater, LCu; 16  $\mu\text{g L}^{-1}$ , MCu; 32  $\mu\text{g L}^{-1}$ , HCu). For each parameter, the value of the control (closed circle) is set as 1.

systems. The D1 protein, as a vital component of the photoreaction center, bears the pressure of photooxidation; excessively high concentrations of Cu may make it more susceptible to damage<sup>35,36</sup>. Damage to the D1 protein has direct consequences on the photosynthetic efficiency of macroalgae, subsequently affecting algal growth and Yield<sup>37</sup>.

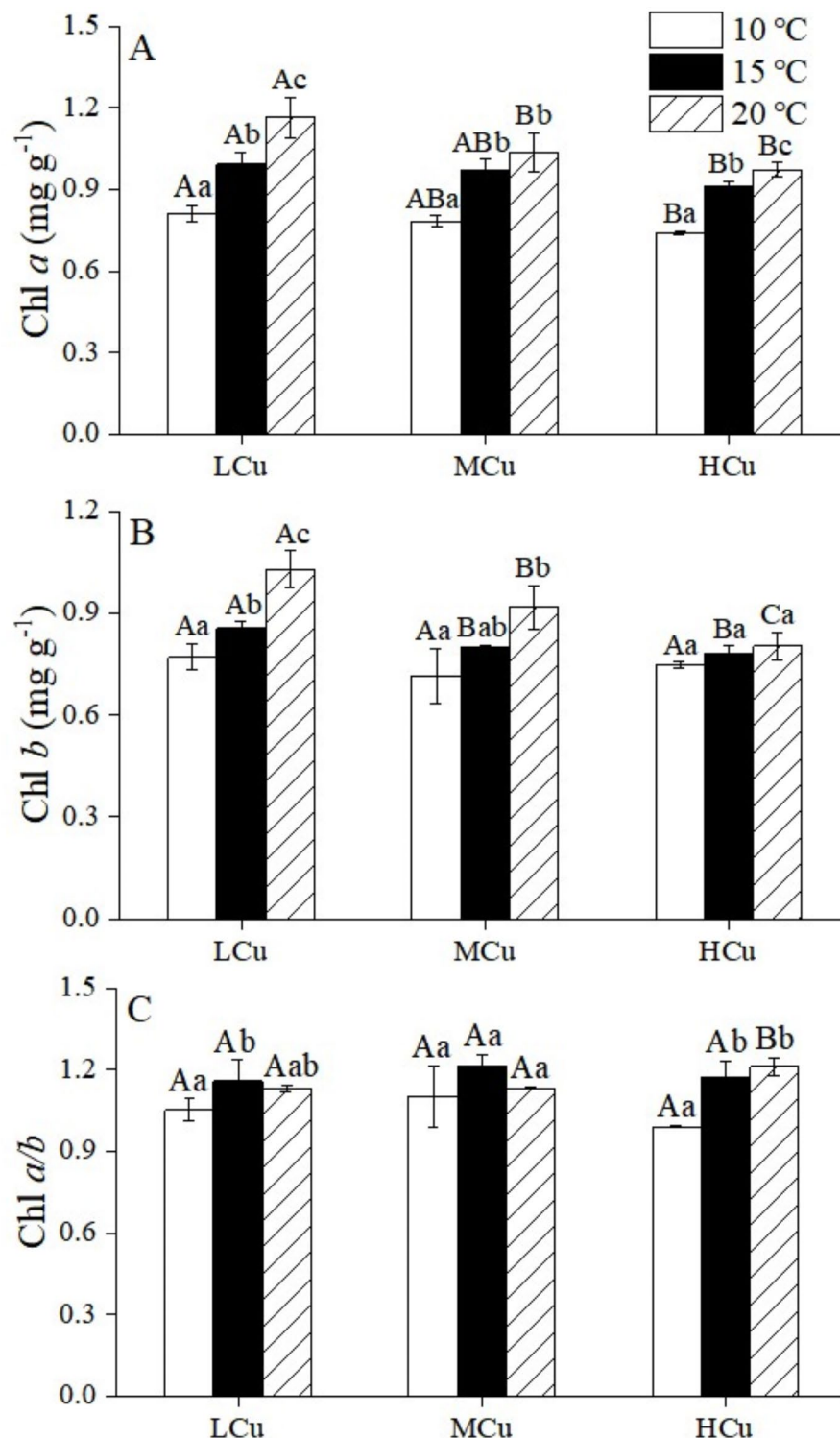


**Fig. 6.** The contents of Chl *a* (A), Chl *b* (B), and Chl *a/b* rate (C) of *U. lactuca* at different temperatures (10 °C, 15 °C, and 20 °C) and Cu concentrations (natural seawater, LCu; 16 µg L<sup>-1</sup>, MCu; 32 µg L<sup>-1</sup>, HCu). Values represent the mean ± SD (n = 3). Different letters represent significant differences ( $P < 0.05$ ) between different Cu concentrations at the same CO<sub>2</sub> concentration. Uppercase letters indicate the analysis of variance for each parameter under different Cu concentrations at the same temperature, while lowercase letters indicate the analysis of variance for each parameter under different temperatures at the same Cu concentration. The horizontal line indicated significant differences among CO<sub>2</sub> concentrations while maintaining the same Cu concentrations ( $P < 0.05$ ).

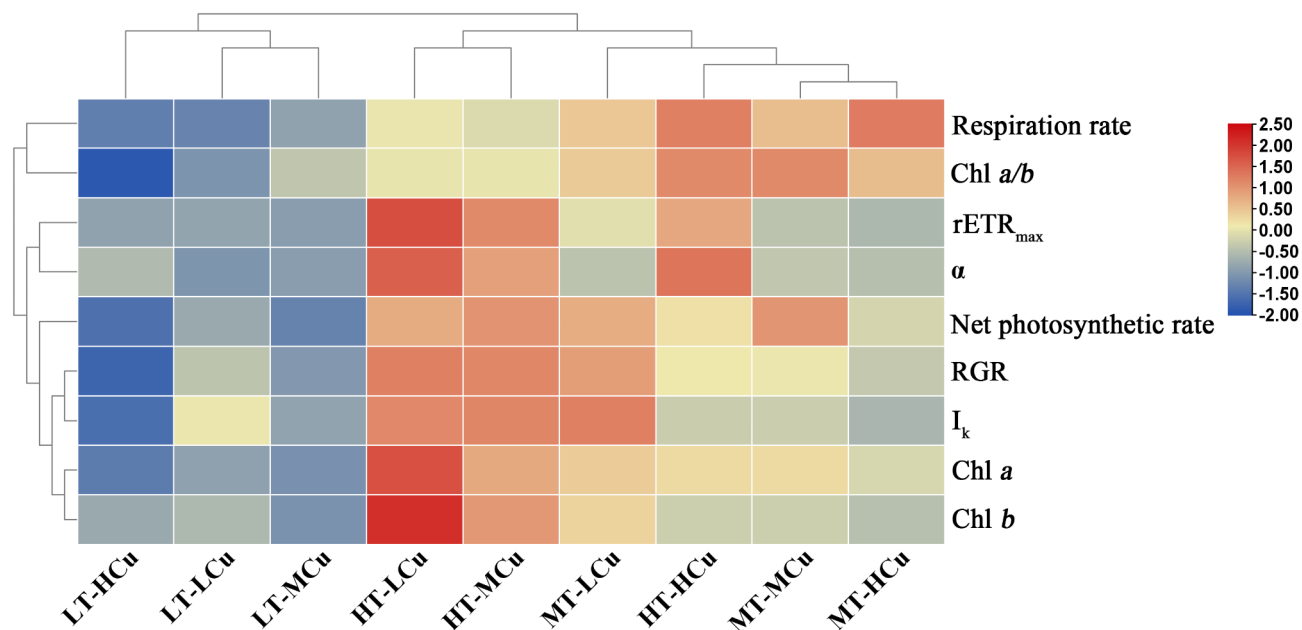


**Fig. 7.** Cluster heatmap analysis of the relative growth rate, net photosynthetic rate, respiration rate, Chl *a* content, Chl *b* content, Chl *a/b* ratio, maximum relative electron transport rate (rETR<sub>max</sub>), electron transport efficiency (α), and saturating irradiance (I<sub>k</sub>) of *U. lactuca* under different temperatures (10 °C, low temperature, LT; 15 °C, medium temperature, MT; 20 °C, high temperature, HT) and Cu concentrations (natural seawater, LCu; 16 μg L<sup>-1</sup>, MCu; 32 μg L<sup>-1</sup>, HCu).

Under conditions of 10 °C, the net photosynthetic rate of thalli decreased with increasing Cu concentration, which was consistent with the RGR results, indicating that the growth of thalli was suppressed by Cu concentration. In the conditions of 15 °C and 20 °C, there were no significant differences in the net photosynthetic rate between the LCu and MCu conditions, but both were higher than the net photosynthetic rate under HCu conditions, which was roughly similar to the RGR results, indicating that high concentrations of Cu inhibit the photosynthetic rate of thalli, thereby suppressing its growth. This might be due to the toxicity of Cu primarily affecting photosynthesis; when the Cu concentration in seawater was too high, Cu could replace Fe to form a “sulfur-iron cluster”, leading to electron overflow, which impacted the photosynthesis and respiration of algal, causing cellular damage<sup>38</sup>. The respiration rate of thalli reached its peak under HCu conditions at 15 °C and 20 °C, further illustrating that respiration could dissipate excess energy within algal, mitigating Cu-induced damage. This result was consistent with research by Jiang et al.<sup>39</sup>, which found that when treating thalli with three concentrations of Cd, increasing Cd concentrations significantly raised the respiration rate while pigment content decreased, indicating an increased energy demand for detoxifying heavy metals. The effect of heavy metal Cd on the growth of thalli may be linked to the suppression of pigment synthesis, downregulation of light energy utilization efficiency, reduction in photosynthetic rate, and increased respiration rate, subsequently leading to a decrease in organic matter accumulation and inhibited growth. Temperature and Cu had significant effects on the photosynthetic activity of *Scenedesmus quadricauda*<sup>40</sup>. Cu reduced the Fv/Fm ratio, increased the production of reactive oxygen species (ROS), and caused severe physiological damage to the cells.

Under three identical temperature conditions, both Chl *a* and Chl *b* showed a decreasing trend with increasing Cu concentration. The reduction in chlorophyll content might be due to heavy metals causing chlorophyll denaturation, preventing photons from being absorbed and transferred to the reaction center<sup>39</sup>. This experiment is consistent with the findings of Hindarti<sup>41</sup>, where the content of Chl *a* and carotenoids in *Nitzschia* sp. decreased after treatment with heavy metals Cu and Cd. In this study, under LCu, MCu, and HCu conditions, the content of Chl *a* and Chl *b* increased with rising temperatures, suggesting that temperature alleviated the toxic effects of Cu on *U. lactuca*. Huang<sup>42</sup> studied *Chlorella* and found that at low temperatures, the damage from membrane lipid peroxidation was greater than at high temperatures. High temperatures could promote the synthesis of superoxide dismutase in the antioxidant enzyme system, while low temperatures enhance the synthesis of catalase, indicating that the varying sensitivity of different antioxidant enzymes to temperature ensures the antioxidant capacity of algal cells at different temperatures<sup>42</sup>. At 10 °C, the rETR<sub>max</sub> and I<sub>k</sub> were highest under low Cu treatment, indicating the highest potential maximum relative electron transfer efficiency and tolerance to strong light. Under HCu, the efficiency of light energy utilization was highest, but the tolerance to strong light was lowest; at 15 °C and 20 °C, the relative electron transfer rate was highest under low Cu treatment and lowest under HCu. The increase in temperature improved the efficiency of light energy utilization, leading to an increase in chlorophyll content and enhanced photosynthesis, thereby increasing the RGR of *U. lactuca*. This was similar to the findings of Huang<sup>43</sup>, which indicated that low temperatures, along with high light exposure at low temperatures, might cause the closure of the PSII reaction center in *Gracilaria*, reducing PSII

activity and effective light energy conversion efficiency, ultimately inhibiting algal growth to a certain extent. The OJIP curve primarily demonstrates the changes in fluorescence at various points of the sample, reflecting variations in the primary photochemical reactions of PSII, as well as changes in the structure and state of the photosynthetic system. In this study, after 20 min of dark treatment, the OJIP curve of *U. lactuca* showed an overall upward trend. Under 10 °C conditions, MCu and LCu had a significant impact on the OJIP curve of *U. lactuca*, with  $DI_0/RC$ ,  $RE_0/RC$ , and  $ABS/RC$  all higher than LCu, indicating that increased Cu concentration stressed the reaction center, increasing its thermal dissipation energy. This might be due to high concentrations of heavy metal stress damaging the reaction active center of PSII, reducing the number of active centers and causing some to close, while also inhibiting electron transfer from PSII  $Q_A^-$  to the PQ pool, resulting in toxicity to both the electron donors on the donor side and the electron acceptors on the acceptor side of PSII, thereby suppressing photosynthesis<sup>42</sup>. In this study, with increasing temperature, the parameters of the PSII reaction center in thalli also continuously increased, indicating that temperature promoted the activity of the PSII reaction center, thereby enhancing photosynthesis. This is consistent with the findings of Zhong et al.<sup>14</sup>, demonstrating that PSII's ability to transfer electrons downstream through the electron chain strengthens, increasing the energy captured from light used for electron transfer.

The clustered heatmap thoroughly analyzed the growth and photosynthetic physiological parameters of *U. lactuca* under varying temperature and Cu concentration conditions. It was evidenced that when high temperature and elevated Cu concentration occurred simultaneously, parameters such as net photosynthetic rate, RGR, and  $rETR_{max}$  significantly declined, respiratory rate peaks, and the Chl *a/b* ratio increased, indicating that the algae entered an irreversible stress state characterized by energy metabolism imbalance. In all low-temperature treatments (10 °C),  $I_k$  and Chl *b* content significantly decreased, and the variation in Cu concentration (LCu, MCu, HCu) had a lesser impact on them. Low temperature combined with high Cu further inhibited photosynthesis (net photosynthetic rate color scale – 2) and growth (RGR color scale – 2.0), but stress response parameters (such as respiratory rate) did not significantly increase, indicating that low temperature itself was the primary cause of physiological inhibition in the algae. Under MT-MCu conditions, photosynthetic parameters fell between those of LT-LCu and HT-HCu, demonstrating that a medium temperature environment could partially mitigate the effects of Cu stress. However, medium Cu still resulted in a slight decrease in photosynthetic efficiency, suggesting a nonlinear interaction between Cu toxicity and temperature.

## Conclusions

At the same temperature, the RGR of *U. lactuca* significantly decreased with increasing Cu concentration. However, under the same Cu concentration conditions, the RGR of the algae gradually increased with rising temperatures. Furthermore, compared to the net photosynthesis rate and chlorophyll content at 10 °C, the increase in net photosynthesis rate and chlorophyll content at 15 °C and 20 °C under low Cu concentration conditions were significantly smaller than the decreases observed at the same temperatures under high Cu concentration conditions. These results indicated that high concentrations of Cu inhibit algal growth at the same temperature, while a moderate increase in temperature could alleviate the toxic effects of Cu on the algae under the same Cu treatment. Such findings not only help us understand the adaptability of *U. lactuca* to environmental stress but also reveal the vulnerability and resilience of marine ecosystems in the face of pollution and climate change.

## Data availability

The datasets used and/or analyzed during the current study are available from the corresponding author on reasonable request.

Received: 22 October 2024; Accepted: 13 March 2025

Published online: 21 March 2025

## References

1. Wunderli-Ye, H. & Solioz, M. *Copper Homeostasis in Enterococcus hirae* Vol. 448, 255–264 (Springer, 1999).
2. Moenne, A., González, A. & Sáez, C. A. Mechanisms of metal tolerance in marine macroalgae, with emphasis on copper tolerance in *Chlorophyta* and *Rhodophyta*. *Aquat. Toxicol.* **176**, 30–37 (2016).
3. Raven, J. A., Evans, M. C. W. & Korb, R. E. The role of trace metals in photosynthetic electron transport in  $O_2$ -evolving organisms. *Photosynth. Res.* **60**, 111–150 (1999).
4. Gao, K. S. & McKinley, K. R. Use of macroalgae for marine biomass production and  $CO_2$  remediation: A review. *J. Appl. Phycol.* **6**, 45–60 (1994).
5. Song, J. M., Li, X. G., Yuan, H. M., Zheng, G. X. & Yang, Y. F. Carbon fixed by phytoplankton and cultured algae in China coastal seas. *Acta Ecol. Sin.* **28**, 551–558 (2008).
6. Zhang, J. H., Fang, J. G. & Tang, Q. S. The contribution of shellfish and seaweed mariculture in China to the carbon cycle of coastal ecosystem. *Adv. Earth Sci.* **20**, 359–365 (2005).
7. Trenberth, K. E., Fasullo, J. T., Von, S. K. & Cheng, L. Insights into Earth's energy imbalance from multiple sources. *J. Clim.* **29**, 7495–7505 (2016).
8. Soler, G. A. et al. Warming signals in temperate reef communities following more than a decade of ecological stability. *Proc. Biol. Sci.* **289**, 20221649 (2022).
9. Davison, I. R. Environmental effects on algal photosynthesis: Temperature. *J. Physiol.* **27**, 2–8 (1991).
10. Zou, D. H. & Xia, J. R. Nutrient metabolism of marine macroalgae and its relationship with coastal eutrophication: A review. *Chin. J. Ecol.* **30**, 589–595 (2011).
11. Tait, L. W. & Schiel, D. R. Impacts of temperature on primary productivity and respiration in naturally structured macroalgal assemblages. *PLoS ONE* **8**, e74413. <https://doi.org/10.1371/journal.pone.0074413> (2013).
12. Li, X. C., Cui, Y. A. & Lei, Y. Z. The effect of primary environmental factors on the purification efficiency of *Ulva pertusa* Kjellman. *Trans. CSAE* **13**, 192–195 (1997).



13. Luan, Q., Lü, F., Wu, H. Y., Ding, G. & Zhan, D. M. Effects of culture conditions on nutrient composition of *Sargassum horneri*. *Prog. Fish. Sci.* **40**, 123–130 (2019).
14. Zhong, Z. H. et al. Ocean acidification exacerbates the inhibition of fluctuating light on the productivity of *Ulva prolifera*. *Mar. Pollut. Bull.* **175**, 113367 (2022).
15. Li, H., Liu, J., Zhang, L. & Tong, P. Effects of low temperature stress on the antioxidant system and photosynthetic apparatus of *Kappaphycus alvarezii* (Rhodophyta, Solieriaceae). *Mar. Biol. Res.* **12**, 1064–1077 (2016).
16. Shin, H. et al. Genome-wide transcriptome analysis revealed organelle specific responses to temperature variations in algae. *Sci. Rep.* **6**, 37770 (2016).
17. Pappou, S., Valsamidis, M. A. & Batjakas, J. B. V. Antibacterial activity of *Ulva lactuca* against important aquaculture bacterial strains. *Bull. Univ. Agric. Sci. Vet. Med. Cluj-Napoca Food Sci. Technol.* **80**, 119–126 (2023).
18. Wang, W. et al. Effect of copper and temperature on the photosynthetic physiological characteristics of *Ulva linza* under elevated CO<sub>2</sub> concentrations. *Mar. Pollut. Bull.* **208**, 116948. <https://doi.org/10.1016/j.marpolbul.2024.116948> (2024).
19. Ma, J., Xu, T. P., Bao, M. L., Zhou, H. M. & Xu, J. T. Response of the red algae *Pyropia yezoensis* grown at different light intensities to CO<sub>2</sub>-induced seawater acidification at different life cycle stages. *Algal Res.* **49**, 101950. <https://doi.org/10.1016/j.algal.2020.101950> (2020).
20. Wei, Y. Q. et al. Different responses of phytoplankton and zooplankton communities to current changing coastal environments. *Environ. Res.* **215**, 114426. <https://doi.org/10.1016/j.envres.2022.114426> (2022).
21. Chakraborty, S. & Owens, G. Metal distributions in seawater, sediment and marine benthic macroalgae from the South Australian coastline. *Int. J. Environ. Sci. Technol.* **11**, 1259–1270 (2014).
22. Wang, Y. J. et al. Environmental impact and recovery of the Bohai Sea following the 2011 oil spill. *Environ. Pollut.* **263**, 114343. <https://doi.org/10.1016/j.envpol.2020.114343> (2020).
23. Xu, T. P. et al. Response of the photosynthetic physiology of *Ulva lactuca* to Cu toxicity under ocean acidification. *Aquat. Toxicol.* **279**, 107222. <https://doi.org/10.1016/j.aquatox.2024.107222> (2025).
24. Jassby, A. D. & Platt, T. Mathematical formulation of the relationship between photosynthesis and light for phytoplankton. *Limnol. Oceanogr.* **21**, 540–547 (1976).
25. Eilers, P. H. C. & Peeters, J. C. H. A model for the relationship between light intensity and the rate of photosynthesis in phytoplankton. *Ecol. Model.* **42**, 199–215 (1988).
26. Porra, R. J., Thompson, W. A. & Kriedemann, P. E. Determination of accurate extinction coefficients and simultaneous equations for assaying chlorophylls a and b extracted with four different solvents: Verification of the concentration of chlorophyll standards by atomic absorption spectroscopy. *BBA Bioenerg.* **975**, 384–394 (1989).
27. Chen, C. et al. TBtools-II: A “one for all, all for one” bioinformatics platform for biological big-data mining. *Mol. Plant.* **16**, 1733–1742 (2023).
28. Akcali, I. & Kucuksezgin, F. A biomonitoring study: Heavy metals in macroalgae from eastern Aegean coastal areas. *Mar. Pollut. Bull.* **62**, 637–645 (2011).
29. Jiang, H. P., Gao, B. B., Li, W. H., Zhu, M. & Wang, C. H. Physiological and biochemical responses of *Ulva prolifera* and *Ulva linza* to cadmium stress. *Sci. World J.* **2013**, 289537. <https://doi.org/10.1155/2013/289537> (2013).
30. Xiao, X. F. et al. Responses and tolerance mechanisms of microalgae to heavy metal stress: A review. *Mar. Environ. Res.* **183**, 105805 (2023).
31. Kondzior, P. & Butarewicz, A. Effect of heavy metals (Cu and Zn) on the content of photosynthetic pigments in the cells of algae *Chlorella vulgaris*. *J. Ecol. Eng.* **19**, 18–28 (2022).
32. Bajguz, A. An enhancing effect of exogenous brassinolide on the growth and antioxidant activity in *Chlorella vulgaris* cultures under heavy metals stress. *Environ. Exp. Bot.* **68**, 175–179 (2010).
33. Han, T., Kang, S. H., Park, J. S., Lee, H. K. & Brown, M. T. Physiological responses of *Ulva pertusa* and *U. armoricana* to copper exposure. *Aquat. Toxicol.* **86**, 176–184 (2008).
34. Leal, P. P. et al. Copper pollution exacerbates the effects of ocean acidification and warming on kelp microscopic early life stages. *Sci. Rep.* **8**, 14763. <https://doi.org/10.1038/s41598-018-32899-w> (2018).
35. Macarena, M., Rodrigo, A. C., Alberto, G., Geraldine, D. & Alejandra, M. Copper-induced synthesis of ascorbate, glutathione and phytochelatins in the marine alga *Ulva compressa* (Chlorophyta). *Plant Physiol. Bioch.* **51**, 102–108 (2012).
36. Gao, G. et al. Expected CO<sub>2</sub>-induced ocean acidification modulates copper toxicity in the green tide alga *Ulva prolifera*. *Environ. Exp. Bot.* **135**, 63–72 (2017).
37. Kumar, S. K. et al. Algal photosynthetic responses to toxic metals and herbicides assessed by chlorophyll a fluorescence. *Ecotox. Environ. Safe* **104**, 51–71 (2014).
38. Li, Q. R., Pi, S., Li, X., Zhou, M. & Liu, C. F. Photosynthetic and stress resistance responses in macroalgae *Ulva pertusa* and *Neopyropia yezoensis* exposed to Cu(II). *Environ. Ecol.* **4**, 47–52 (2022).
39. Jiang, Y. Y., Jin, P., Zeng, X. P., Wei, Y. Y. & Xia, J. R. Ocean acidification affects the physiological toxicity of the heavy metal Cd on *Ulva*. *J. Guangzhou Univ. Nat. Sci. Ed.* **18**, 80–87 (2019).
40. Yong, W. K. et al. Interactive effects of temperature and copper toxicity on photosynthetic efficiency and metabolic plasticity in *Scenedesmus quadricauda* (Chlorophyceae). *J. Appl. Phycol.* **30**, 3029–3041 (2018).
41. Hindarti, D. & Larasati, A. W. Copper (Cu) and Cadmium (Cd) toxicity on growth, chlorophyll-a and carotenoid content of phytoplankton *Nitzschia* sp. *IOP Conf. Ser. Earth Environ. Sci.* **236**, 012053 (2019).
42. Huang, L. Q. Effect of temperature and heavy metal stress on *Chlorella* growth and key enzymes. *Chongqing Sanxia Inst.* **18**, 351–359 (2021).
43. Huang, Y. J. et al. Photophysiological responses of *Gracilariopsis bailinae* to temperature and light intensity. *South China Fish. Sci.* **19**, 139–147 (2023).

## Acknowledgements

This study was supported by the Special Fund for Natural Resources Development of Jiangsu Province (JSZ-RHYKJ202206), Chinese National Natural Science Foundation (No. 42106089), Key Project of Natural Science of Jiangsu High School, Grant/Award (No. 21KJA170001), and the Priority Academic Program Development of Jiangsu Higher Education Institutions, Jiangsu Qinglan, Lianyungang 521 Talent Projects (LYG06521202397 and LYG06521202129), and Postgraduate Research and Practice Innovation Program of Jiangsu Province (KYCX23\_3449), and Lianyungang Municipal Science and Technology Program—Key R&D Program (Social Development) (SF2433).

## Author contributions

Each author has contributed to this article. Jing Ma, Yuxin Xie, Cheng Chen, and Juntian Xu designed the experimental scheme; Yuxin Xie, Wenjing Ge, Houxu Ding, Yaping Wu, Zhouyue Lu, and Xiangwen Bao performed the laboratory tests and processed the experimental data; Jing Ma, Yuxin Xie, and Guoqiang Chen drafted and revised the paper; Juntian Xu improved the paper's structure and language. All authors reviewed the manuscript.

## Declarations

### Competing interests

The authors declare no competing interests.

### Additional information

**Correspondence** and requests for materials should be addressed to J.X.

**Reprints and permissions information** is available at [www.nature.com/reprints](http://www.nature.com/reprints).

**Publisher's note** Springer Nature remains neutral with regard to jurisdictional claims in published maps and institutional affiliations.

**Open Access** This article is licensed under a Creative Commons Attribution-NonCommercial-NoDerivatives 4.0 International License, which permits any non-commercial use, sharing, distribution and reproduction in any medium or format, as long as you give appropriate credit to the original author(s) and the source, provide a link to the Creative Commons licence, and indicate if you modified the licensed material. You do not have permission under this licence to share adapted material derived from this article or parts of it. The images or other third party material in this article are included in the article's Creative Commons licence, unless indicated otherwise in a credit line to the material. If material is not included in the article's Creative Commons licence and your intended use is not permitted by statutory regulation or exceeds the permitted use, you will need to obtain permission directly from the copyright holder. To view a copy of this licence, visit <http://creativecommons.org/licenses/by-nc-nd/4.0/>.

© The Author(s) 2025